Constrained high-order statistical blind deconvolution of spectral data

Jinghe Yuan (袁景和)[1], Ziqiang Hu (胡自强)[1], Guiying Wang (王桂英)[2], and Zhizhan Xu (徐至展)[2]

[1] *Institute of Science and Technology for Opto-Electron Information, Yantai University, Yantai 264005*

[2] *Shanghai Institute of Optics and Fine Mechanics, Chinese Academy of Sciences, Shanghai 201800*

Received March 21, 2005

A constrained high-order statistical algorithm is proposed to blindly deconvolute the measured spectral data and estimate the response function of the instruments simultaneously. In this algorithm, no prior-knowledge is necessary except a proper length of the unit-impulse response. This length can be easily set to be the width of the narrowest spectral line by observing the measured data. The feasibility of this method has been demonstrated experimentally by the measured Raman and absorption spectral data.

OCIS codes: 300.6320, 300.6450, 300.1030.

The spectra recorded by dispersion spectrophotometer are usually distorted by the response function of the instrument. These distortions generally include the overlapping of adjacent peaks and the aberrancy of the relative intensities among the peaks. The major factor of the instrument response function limiting the resolving power is the slit width and the diffractive limit of the dispersive grating. To improve the resolving power, double or triple cascade spectrophotometer, narrow slits have been employed, but the total flux of the available radiation decreases accordingly, resulting in a low signal-to-noise ratio (SNR), a longer measuring time, and a larger expenditure. Hence, there is a trade-off among the resolving power, the SNR, the measuring time, and the instrument expenditure. The impulse response of electronic circuits also degrades the spectral resolution. Otherwise, spectral resolution can be significantly improved by mathematically removing the effect of the instrument response function. This is the mission of the deconvolution. The most popular method for resolving this problem is Wiener filtering[1]. But the blind deconvolution is a more challenging task because the actual data and the instrument response function must be estimated simultaneously from the measured data. Homomorphic filtering based method developed by Senga *et al.*[1] was applied to infrared molecular absorption spectra successfully. But this method needs to calculate the logarithm of the Fourier spectrum, which is time-costly, and is limited to the cases where the slit function is triangle. The Jansson algorithm[2] starting from an initial guess of the instrument response function estimates the actual data iteratively. But the choice of the convolution kernel is often reasonless.

In this letter, based on the central limit theorem and the universal methods for blind deconvolution of communication signals developed in Ref. [3], a high-order statistical blind deconvolution algorithm is proposed. The measured spectral data experimentally demonstrate the feasibility of this method.

For a digital measured spectral data series

$$\mathbf{X} = (x(1), x(2), \cdots, x(N))^T, \tag{1}$$

which is the convolution of the actual spectral data and the instrument response function

$$x(n) = \sum_{k=0}^{Q} f_k w(n-k), \quad n = 1, 2, \cdots, N, \tag{2}$$

where $\mathbf{W} = (w(1), w(2), \cdots, w(n))^T$ is the actual data, and $\mathbf{F} = (f_0, f_1, \cdots, f_Q)^T$ is the unit-impulse response of measure instruments.

To find a suitable deconvolution operator $\mathbf{G} = (g_0, g_1, \cdots, g_Q)^T$, let

$$y(n) = \sum_{k=0}^{Q} g_k x(n-k), \quad n = 1, 2, \cdots, N, \tag{3}$$

and

$$y(n) = aw(n-m), \tag{4}$$

where a is an arbitrary nonzero scalar, and m is the space-shift parameter. Namely, the deconvoluted data $\mathbf{Y} = (y(1), y(2), \cdots, y(N))^T$ should be a scaled and space-shifted image of the actual data $\mathbf{W}$. So the cascade of the convolution and deconvolution operation should satisfy

$$h_n = \sum_{k=0}^{Q} f_k g_{n-k} = a\delta(n-m), \tag{5}$$

where $\{\delta(n)\}$ denote the Kronecker delta series defined by

$$\delta(n) = \begin{cases} 1, & n = 0 \\ 0, & \text{otherwise} \end{cases}.$$

Because all the spectral data are real value, referring to the deconvolution criteria in Ref. [4], we only need to find a suitable $\mathbf{G}$ to satisfy following deconvolution criterion

$$\max |c_Y(p,q)| \quad \text{subject to} \quad c_Y(2) = c_W(2), \tag{6}$$

where $|c_Y(p,q)|$ is the amplitude of the (p,q)-order normalized cumulant of $\mathbf{Y}$, and $c_Y(2)$, $c_W(2)$ are the 2-order

cumulants (variance) of $\mathbf{Y}$ and $\mathbf{W}$, respectively. In practical applications, $p = 6$, $q = 2$ is a good choice, so we will calculate the (6,2)-order normalized cumulant in this letter.

To find a suitable unit-impulse response $\mathbf{G}$, so as to maximize the amplitude of the (6,2)-order normalized cumulant, the steepest ascent algorithm is a general selection. The mth approximation of $\mathbf{G}$ is updated as

$$\mathbf{G}_{m+1} = \mathbf{G}_m + \alpha \mathbf{d}, \quad m = 0, 1, 2, \cdots, \tag{7}$$

where α is a proper positive scalar and $\mathbf{d}$ is an update vector.

So as

$$\left|\hat{c}\,(6,2)^{(m+1)}\right| > \left|\hat{c}_Y\,(6,2)^{(m)}\right|, \tag{8}$$

where $\left|\hat{c}_Y\,(6,2)^{(m)}\right|$ is the (6,2)-order normalized cumulant amplitude of the estimate $\hat{\mathbf{Y}}$ with $\mathbf{G}_m$.

Let the gradient vector of the (6,2)-order normalized cumulant amplitude with respect to $\mathbf{G}_m$ as the update vector $\mathbf{d}$. Because $|\hat{c}_Y\,(6,2)| = \hat{c}_Y\,(6,2)\,\mathrm{sgn}\,[\hat{c}_Y\,(6,2)]$, we only need to estimate the (6,2)-order normalized cumulant $\hat{c}_Y\,(6,2)$

$$\hat{c}_Y\,(6,2) = \frac{\hat{\mu}_Y\,(6) - 15\hat{\mu}_Y\,(4)\,\hat{\mu}_Y\,(2) - 10\hat{\mu}_Y\,(3)^2 + 30\hat{\mu}_Y\,(2)^3}{\hat{\mu}_Y\,(2)^3}, \tag{9}$$

where $\hat{\mu}_Y\,(k)$ is the k-order central moments of $\hat{\mathbf{Y}}$ defined by

$$\hat{\mu}_Y\,(k) = \frac{1}{N-Q}\sum_{n=Q+1}^{N}\left[\hat{y}\,(n) - \hat{m}_Y\right]^k, \quad k = 1, 2, \cdots, \tag{10}$$

and the mean $\hat{m}_Y$ is

$$\hat{m}_Y = \frac{1}{N-Q}\sum_{n=Q+1}^{N}\hat{y}\,(n). \tag{11}$$

Hence, the gradient vector of the (6,2)-order normalized cumulant with respect to $\mathbf{G}_m$ is

$$\begin{aligned}\frac{\partial \hat{c}_Y\,(6,2)}{\partial g_t} = {} & \frac{1}{\hat{\mu}_Y\,(2)^3}\frac{\partial\left[\hat{\mu}_Y\,(6)\right]}{\partial g_t} - \frac{15}{\hat{\mu}_Y\,(2)^2}\frac{\partial\left[\hat{\mu}_Y\,(4)\right]}{\partial g_t} - \frac{20\hat{\mu}_Y\,(3)}{\hat{\mu}_Y\,(2)^3}\frac{\partial\left[\hat{\mu}_Y\,(3)\right]}{\partial g_t} \\ & - \frac{3\hat{\mu}_Y\,(6) + 30\hat{\mu}_Y\,(4)\,\hat{\mu}_Y\,(2) - 30\hat{\mu}_Y\,(3)^2}{\hat{\mu}_Y\,(2)^4}\frac{\partial\left[\hat{\mu}_Y\,(2)\right]}{\partial g_t}, \quad t = 0, 1, \cdots, Q.\end{aligned} \tag{12}$$

Let $k = 6, 4, 3, 2$ respectively in Eq. (10), and substitute it into Eq. (12), we obtain

$$\begin{aligned}\frac{\partial \hat{c}_Y\,(6,2)}{\partial g_t} = {} & \frac{6}{(N-Q)\,\hat{\mu}_Y\,(2)^3}\sum_{n=Q+1}^{N}\left\{\left[\hat{y}\,(n) - \hat{m}_Y\right]^5\left[x\,(n-t) - \frac{1}{(N-Q)}\sum_{k=Q+1}^{N}x\,(k-t)\right]\right\} \\ & - \frac{60}{(N-Q)\,\hat{\mu}_Y\,(2)^2}\sum_{n=Q+1}^{N}\left\{\left[\hat{y}\,(n) - \hat{m}_Y\right]^3\left[x\,(n-t) - \frac{1}{(N-Q)}\sum_{k=Q+1}^{N}x\,(k-t)\right]\right\} \\ & - \frac{60\hat{\mu}_Y\,(3)}{(N-Q)\,\hat{\mu}_Y\,(2)^3}\sum_{n=Q+1}^{N}\left\{\left[\hat{y}\,(n) - \hat{m}_Y\right]^2\left[x\,(n-t) - \frac{1}{(N-Q)}\sum_{k=Q+1}^{N}x\,(k-t)\right]\right\} \\ & - \frac{6\hat{\mu}_Y\,(6) - 60\hat{\mu}_Y\,(4)\,\hat{\mu}_Y\,(2) - 60\hat{\mu}_Y\,(3)^2}{(N-Q)\,\hat{\mu}_Y\,(2)^4}\sum_{n=Q+1}^{N}\left\{\left[\hat{y}\,(n) - \hat{m}_Y\right]\left[x\,(n-t) - \frac{1}{(N-Q)}\sum_{k=Q+1}^{N}x\,(k-t)\right]\right\}, \\ & t = 0, 1, \cdots, Q.\end{aligned} \tag{13}$$

If $\mathbf{X}$ is of zero-mean (it is always realizable) and $N - Q$ is large enough, we will have

$$\frac{1}{(N-Q)}\sum_{k=Q+1}^{N}x\,(k-t) \approx 0, \quad t = 0, 1, \cdots, Q. \tag{14}$$

Hence

$$\frac{\partial \hat{c}_Y(6,2)}{\partial g_t} = \frac{6}{(N-Q)\hat{\mu}_Y(2)^3}\sum_{n=Q+1}^{N}\left\{[\hat{y}(n)-\hat{m}_Y]^5 x(n-t)\right\} - \frac{60}{(N-Q)\hat{\mu}_Y(2)^2}\sum_{n=Q+1}^{N}\left\{[\hat{y}(n)-\hat{m}_Y]^3 x(n-t)\right\} - \frac{60\hat{\mu}_Y(3)}{(N-Q)\hat{\mu}_Y(2)^3}\sum_{n=Q+1}^{N}\left\{[\hat{y}(n)-\hat{m}_Y]^2 x(n-t)\right\} - \frac{6\hat{\mu}_Y(6)-60\hat{\mu}_Y(4)\hat{\mu}_Y(2)-60\hat{\mu}_Y(3)^2}{(N-Q)\hat{\mu}_Y(2)^4}\sum_{n=Q+1}^{N}\left\{[\hat{y}(n)-\hat{m}_Y]x(n-t)\right\}, \quad t=0,1,\cdots,Q. \tag{15}$$

Let $\alpha=(\rho)^k$, $k=0,1,2,\cdots$, and $0<\rho<1$, we can obtain

$$\mathbf{G}_{m+1}=\mathbf{G}_m+(\rho)^k\nabla_{\mathbf{G}}\left[\hat{c}_Y(6,2)^{(m)}\right]\operatorname{sgn}\left[\hat{c}_Y(6,2)^{(m)}\right]. \tag{16}$$

This iteration stops when the gradient vector being sufficiently close to zero or the relative change in (6,2)-order normalized cumulant amplitude being sufficiently small from one loop to the next.

Referring to Ref. [4], the constraint $\hat{c}_Y(2)=c_W(2)$ in the criterion (6) implies that $\left\|\hat{h}\right\|^2=\sum_{k=0}^{Q}\left|\hat{h}_k\right|^2=1$, which can be realized by letting $\mathbf{G}_m=\frac{1}{\sqrt{\mathbf{G}_m^T\mathbf{R}\mathbf{G}_m}}\mathbf{G}_m$, where $\mathbf{R}$ is the a $(Q+1)\times(Q+1)$ matrix whose $(s,\ t)$ element is

$$R_{st}\approx\frac{\operatorname{cov}[x(n-t),x(n-s)]}{\operatorname{var}[x(n)]},\quad s,t=0,1,\cdots,Q. \tag{17}$$

Before applying the algorithm above-supposed to real spectral data, proper update step ρ and length of the unit-impulse-response $Q+1$ should be chosen. The update step ρ influences the convergent speed, and should be set to a larger value (such as $\rho=0.9$) for a stationary convergence behavior. The choice of $Q+1$ influences the deconvolution results dramatically. Too small $Q+1$ may generate some pseudo spectral lines and lead to misanalysis. Too large $Q+1$ may make deficient deconvolution results. In following experiments, we set $Q+1$ equal to the width of the narrowest spectral line by observing the spectral data.

In the algorithm, suppose the input data $\mathbf{X}$ is of zero-mean. We must preprocess it by subtracting its mean, and then plus this mean to the final deconvoluted data. So the input data $\mathbf{X}$ is always supposed to be of zero-mean in the deconvolution operation.

Figure 1(a) is 846 length Raman spectral data of (D+)-glucopyranose[4] from 155 to 1000 cm^{-1}. The spectral resolution is about 4 cm^{-1}. Figure 1(b) is the deconvoluted data. Here we choose $Q=5$, $\rho=0.9$, and $e=10^{-11}$. When the change of $\hat{c}_y(6,2)$ from one loop to the next is less than e, the iteration stops. The peak at 406 cm^{-1} is split into two peaks at 396 and 407 cm^{-1} respectively, and the peak at 542 cm^{-1} is split into two peaks at 541 and 558 cm^{-1} respectively. The relative intensity distortion has also been revised. Figures 1(c) and (d) are the unit-pulse responses for $Q=5$ and $Q=6$, respectively, which are very alike. For $Q=6$, the deconvouted result is identical with Fig. 1(b), and will not be plotted here. From Figs. 1(c) and (d), we can know that the response function of instruments is about 6 in length, and with increasing the length, some small fluctuations appear. Figure 2(a) is 601 length absorption spectral data of Cr:LiSAF crystal[5] from 300 to 900 nm. The two absorption peaks at 631 and 661 nm overlap each other, and only two pinnacles can be distinguished. Figure 2(b) is the deconvoluted data. Here $Q=15$, $\rho=0.9$, and $e=10^{-11}$. The two absorption peaks at 631 and 661 nm are split into four peaks at 579, 603, 631, and 662 nm, respectively. Figures 2(c) and (d) are the unit-pulse responses for $Q=15$ and $Q=20$, respectively, and they are very alike.

By experiments, this statistical method is a feasible blind deconvolution strategy of spectral data. The actual spectral data and the unit-impulse response of the

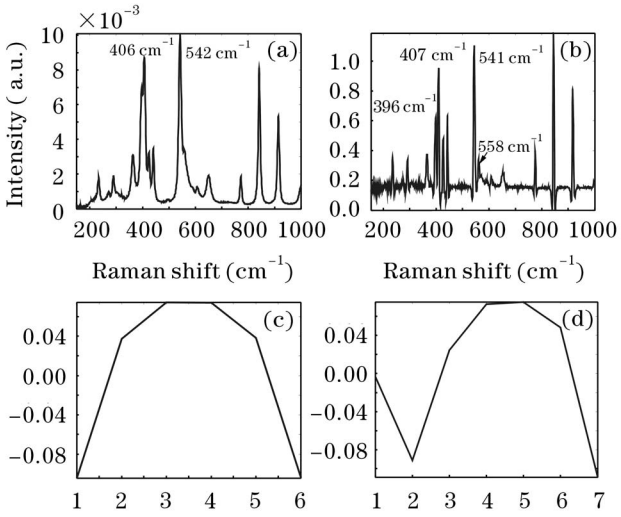

Fig. 1. 846 length Raman data of (D+)-Glucopyranose from 155 to 1000 cm^{-1} (a), the blind deconvoluted data of (a) for $Q=5$, $\rho=0.9$ (b), estimated unit-impulse responses for $Q=5$ (c) and $Q=6$ (d).

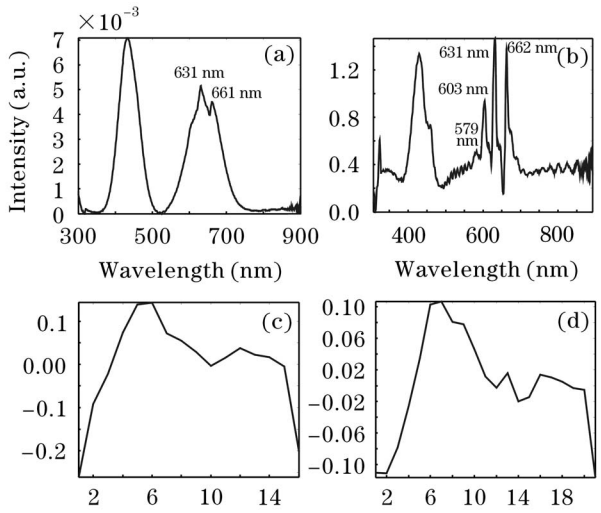

Fig. 2. 601 length absorption spectral data of Cr:LiSAF crystal from 300 to 900 nm (a), blind deconvoluted spectral data of (a) for $Q = 15$, $\rho = 0.9$ (b), estimated unit-impulse responses for $Q = 15$ (c) and $Q = 20$ (d).

measuring instruments can be estimated simultaneously. The spectral resolution can be improved considerably and the distortion of the relative intensity can be revised in some degree. In this method, no more prior-knowledge is necessary and therefore it can be applied to a wide range of spectral blind deconvolution.

J. Yuan's e-mail address is jacobyuan@yahoo.com.cn.

References

1. Y. Senga, K. Minami, S. Kawata, and S. Minami, Appl. Opt. **23,** 1601 (1984).
2. R. D. Davies and P. A. Jansson, *"Applications to electron spectroscopy for chemical analysis"*, in *Deconvolution of Images and Spectra* (2nd edn.) P. A. Jansson (ed.) (Academic Press, San Diego, 1997).
3. O. Shalvi and E. Weinstein, *"Universal Methods for Blind Deconvolution"*, in *Blind Deconvolution* S. Haykin (ed.) (Prentice-Hall, Englewood Cliffs, 1994) pp.122—168.
4. S. B. Engelson, "Raman Spectral of (D+)-Glucopyranose" http://www.models.kvl.dk/users/ergelsen/specarb/glcb.html.
5. NASA, "Absorption Spectral Data of Cr:LiSAF Crystal" http://aesd.larc.nasa.gov/gl/laser/spectra/spectra.htm.